

Received March 21, 2021, accepted March 29, 2021, date of publication April 1, 2021, date of current version April 12, 2021.

Digital Object Identifier 10.1109/ACCESS.2021.3070328

Unbalanced-/Balanced-to-Unbalanced Diplexer Based on Dual-Mode Dielectric Resonator

LIN XU^{1,2}, WEI YU^{1,3}, AND JIAN-XIN CHEN^{1,2}, (Senior Member, IEEE)

¹School of Information Science and Technology, Nantong University, Nantong 226019, China

²Nantong Research Institute for Advanced Communication Technologies, Nantong 226019, China

³Center for Engineering Training, Nantong University, Nantong 226019, China

Corresponding author: Jian-Xin Chen (jxchen@hotmail.com)

This work was supported in part by the National Natural Science Foundation under Grant 62001253, in part by the Natural Science Foundation of Jiangsu under Grant BK20201438, in part by the Natural Science Research Project of Jiangsu Provincial Institutions of Higher Education under Grant 20KJA510002, in part by the Nantong Basic Science Research Program under Grant JC2020080, and in part by the Postgraduate Research and Practice Innovation Program of Jiangsu Province under Grant KYCX18_2420.

ABSTRACT The design of compact unbalanced-/balanced-to- unbalanced diplexer (U2U/B2U) based on full dual-mode dielectric resonator (DR) is investigated for the first time. The relationships of the external quality factors (Q_e) under the two modes are analyzed. It is found that the Q_e of two modes can be controlled independently, which makes the design procedure simple and efficient. Based on the analysis, both of the proposed U2U and B2U diplexer can be easily built by properly adding feeding probes for the DR without increasing the circuit size by altering the location of the feeding probes according to the distribution of the electromagnetic fields. To verify the proposed design concept, the diplexers mentioned above are simulated, implemented and measured. The isolation is achieved by the orthogonality between modes while the low insertion loss is obtained due to the high unloaded quality factor (Q_u) of the dual-mode DR. The measurements are in accordance with the simulated results, showing low loss and good selectivity.


INDEX TERMS Miniaturization, dual-mode dielectric resonator (DR), diplexer, design approach, unbalanced-to-unbalanced (U2U), balanced-to-unbalanced (B2U).

I. INTRODUCTION

With the rapid development of modern wireless communication systems, the features of miniaturization, low insertion loss and high performance are highly desired. As a key component of RF front end, the diplexer is essential in the multi-frequency transceiver [1]. Since a diplexer can simultaneously deal with the uplink and downlink signals, the number of filters can be reduced by half [2]. Due to the aforementioned advantages, various diplexers have been reported. In traditional designs, two independent bandpass filters are combined by a common T-junction which makes that one filter an open circuit at the frequency of the other pass-band [3]–[7]. However, the T-junction needs to be designed individually and occupies additional size. To miniaturize the circuit size, a common dual-mode resonator is used to replace the T-junction and act as the first level of the resonant circuit [8]–[12]. However, since the subsequently cascaded resonators in many reported works are still based on the

single-mode resonator, the advantage of dual-mode resonator for miniaturization is not fully realized. In recent years, the structure based on full dual/multi-mode resonator is proposed by replacing the subsequently cascaded single-mode resonators with dual/multi-mode resonators, which makes further miniaturization achieved [13]–[19]. In [15], a quad-mode resonator is designed and applied to design compact dual-band diplexer. However, since the probe excites four modes simultaneously, the external quality factors (Q_e) under each mode can't be controlled independently, which makes the design procedure complicated. Therefore, how to achieve a balance between miniaturization and design efficiency is worth studying.

On the other hand, most of the works are based on the microstrip and SIW, showing various merits. However, due to the relatively low unloaded quality factor (Q_u) of the resonator, the insertion loss and selectivity of the pass-band are not good. The metal cavity can provide a high Q_u [18]–[21], but the size is bulky. The dielectric resonator (DR) can be treated as a bridge between the microstrip line/SIW and metal cavity resonators in terms of Q_u and

The associate editor coordinating the review of this manuscript and approving it for publication was Abhishek K Jha .

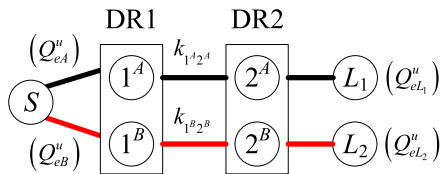


FIGURE 1. Topology of the U2U diplexer.

volume. Accordingly, DR has been widely applied to design microwave circuits [22]–[25]. Among them, the diplexer based on DR also has been reported. In [26] and [27], an off-centered triple-mode DR is proposed to design the diplexer, achieving compact size and low insertion loss.

Balanced circuits, containing high immunity to interference distortion, are widely applied in antennas to achieve symmetrical radiation pattern, high common-mode rejection, low cross polarization, and good impedance matching [28]–[30]. As an interface between the single-ended and balanced components (i.e. the connector between a differential antenna and a receiver/transmitter), the balun diplexer is also highly desired. For the unbalanced-to-balanced (U2B) diplexer, differential signal can be realized by the half-wavelength transmission line [31], [32]. Most of the designs using this approach are based on the microstrip line which often suffers from high loss. For the balanced-to-unbalanced (B2U) diplexer, an effective approach is to excite a pair of differential modes at the input, which is effectively applied in the metal cavity [18]. However, up to now, the B2U diplexer based on DR hasn't been reported.

In this paper, the designs of the U2U and B2U diplexer based on full dual-mode DR are proposed. The full dual-mode structure effectively reduces the circuit size. Meanwhile, the design process is simple and efficient because the Q_e values of the two modes can be controlled independently. The proposed U2U and B2U diplexers can be easily built by properly adding feeding probes for the DR without increasing the circuit size by altering the location of the feeding probes according to the distribution of the electromagnetic fields. Both of the two designs are fabricated and measured for demonstration. Multiple features are achieved, such as compact size, low insertion loss and good selectivity.

II. ANALYSIS OF DR DIPLEXER

Fig. 1 shows the topology of the proposed U2U diplexer. S and L_i ($i = 1, 2$) represent the source and loads. The black and red lines represent the first and second channels. 1^A (2^A) and 1^B (2^B) represent the lower and higher resonant frequencies of the dual-mode DR, respectively. Based on this topology, a U2U diplexer is designed. The structure of the proposed U2U diplexer based on the dual-mode DR is shown in Fig. 2. A metal baffle is located in the middle of the cavity to form two paths for signal transmission. The width of apertures w_1 and w_2 are used to control the coupling coefficient between the two DRs. The probe length and the gap determine the coupling between the port and DR. Port 1 is the input port that excites the dual mode of the DR simultaneously. Port 2 and

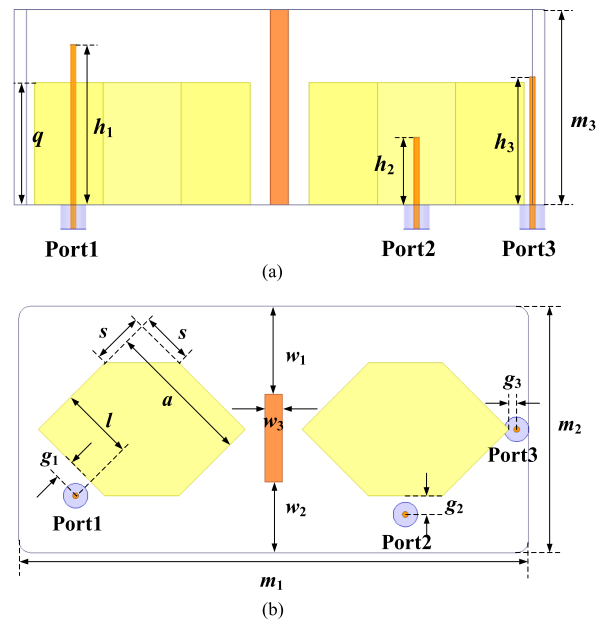


FIGURE 2. Structure of the U2U diplexer: (a) Front view; (b) Top view.

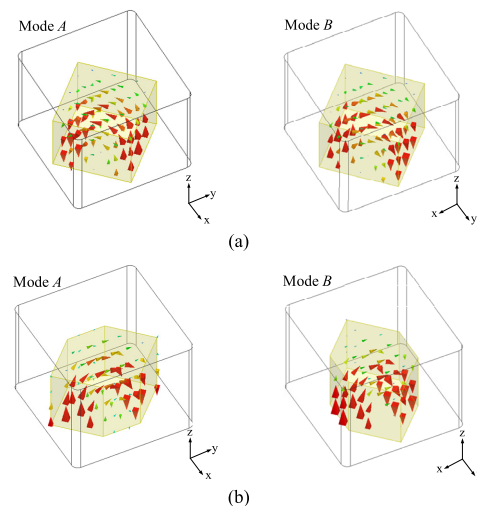


FIGURE 3. E-field distributions of a dual-mode DR cavity. (a) Without and (b) with corner cuts.

Port 3 are the two output ports. The DR is placed at the bottom of the metal cavity which is used as the electrical wall of the dominant mode of the DR.

The DR has the relative dielectric constant $\epsilon_r = 38$ with loss tangent $\tan\delta = 2.5 \times 10^{-4}$. Figs. 3(a) and (b) show the E-fields of the dual-mode DR with or without corner cuts. It can be seen that before the corner cutting where the DR is in square shape, the E-fields of the two modes distribute along the edge as shown in Fig. 3(a) while the E-fields distribute along the diagonal after the corner cutting as shown in Fig. 3(b). In both cases, the two modes are always orthogonal with each other. To excite the two modes separately, the feeding probe should be arranged along the direction of polarization. Fig. 4 shows the relationship between the dual-mode frequencies and the corner cuts. With the increase

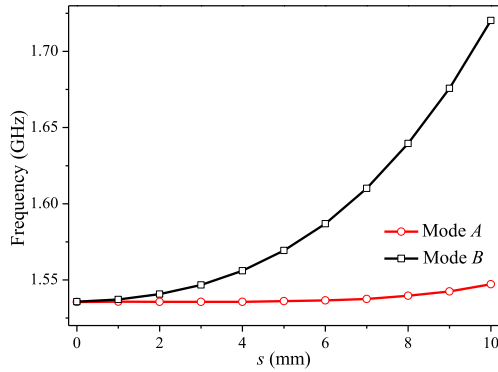


FIGURE 4. Resonant frequencies of Mode A and Mode B versus the corner cuts.

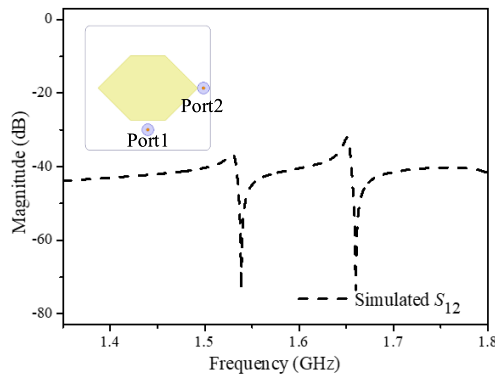


FIGURE 5. The isolation between Mode A and Mode B.

of s , the resonant frequency of Mode A remains unchanged while the frequency of Mode B increases. Fig. 5 shows the isolation between the two modes. Because of the orthogonality between the modes, the isolation between 1.35 GHz and 1.7 GHz is greater than 30 dB, which is suitable for diplexer design.

III. UNBALANCED-TO-UNBALANCED DIPLEXER

Figs. 6(a)-(d) show the Q_e of the three unbalanced ports versus probe location, probe length and the coupling gap between the DR and probe. Figs. 6(a)-(b) show the extracted Q_e at the common input port (port 1) for the two modes (Q_{eA}^u and Q_{eB}^u). It is shown that the two modes can be excited simultaneously and controlled independently, i.e. Q_{eB}^u varies within a small range while the value of Q_{eA}^u can be changed in a large range. Q_{eA}^u increases as l increases or h_1

decreases while Q_{eB}^u keeps almost unchanged from $l = 10$ mm to 18 mm. The similar relationship between Q_{eA}^u (Q_{eB}^u) and l (or g_1) can be obtained. By adjusting the three parameters (l , g_1 , and h_1), the required Q_e can be easily obtained at port 1. Figs. 6(c)-(d) show the extracted Q_e under each of the two modes against different h_2 (h_3) and g_2 (g_3). In this case, the port should be arranged along the corresponding polarization direction as shown in Fig. 3. Fig. 7 shows the coupling coefficient k versus w_1 with different w_2 .

According to the design specification, the lower and higher center frequencies are respectively 1.52 GHz and 1.64 GHz, which corresponds to $s = 8.7$ mm. Through calculation, we obtain $k_{1A2A} = 0.006$ and $Q_{eA}^u = 190.2$ for the lower passband while $k_{1B2B} = 0.0067$ and $Q_{eB}^u = 167$ for the higher passband. Accordingly, the coupling matrix of U2U diplexer can be obtained as shown in (1), as shown at the bottom of the page.

Since there is actually a small amount of coupling between the orthogonal modes and the two output ports, the coupling coefficients of M_{2B1A} and M_{2A1B} are not zero. Fig. 8 shows the theoretical and simulated results with good agreement.

The design procedure of the U2U diplexer can be summarized as follows.

- (1) Calculate the Q_e and the coupling coefficient according to the design specification.
- (2) Select the lengths of the feeding probes and the gap between the feeding probes and DR according to Figs. 6(a)-(d).
- (3) Select the w_1 and w_2 of the metal baffle according to Fig. 7.
- (4) Optimize the dimensions according to the response.

According to the required k and Q_e , the dimensions of the proposed U2U diplexer after optimization can be determined as follows: $m_1 = 83$ mm, $m_2 = 40$ mm, $m_3 = 32$ mm, $a = 25$ mm, $q = 20$ mm, $l = 12.5$ mm, $g_1 = 3$ mm, $g_2 = 3$ mm, $g_3 = 0.8$ mm, $w_1 = 11.8$ mm, $w_2 = 11.8$ mm, $w_3 = 3$ mm, $h_1 = 27.3$ mm, $h_2 = 20$ mm, and $h_3 = 20$ mm. The simulated and measured results are shown in Fig. 9. The center frequencies of the dual band are 1.52 GHz and 1.64 GHz, respectively. The simulated dual-band return losses are better than 18.5 dB and 15.2 dB while the measured return losses are better than 14.5 dB and 14 dB. The simulated dual-band insertion losses are both less than 0.54 dB while the measured insertion losses of the dual bands are both less than 0.8 dB.

$$M = \begin{bmatrix} S & 1^A & 2^A & 1^B & 2^B & L_1 & L_2 \\ S & 0 & 0.2560 & 0 & 0.2740 & 0 & 0 \\ 1^A & 0.2560 & 0.9476 & 0.0750 & 0 & 0 & 0 \\ 2^A & 0 & 0.0750 & 0.9476 & 0 & 0.2560 & 0.003 \\ 1^B & 0.2740 & 0 & 0 & -0.9490 & 0.0840 & 0 \\ 2^B & 0 & 0 & 0 & 0.0840 & -0.0940 & 0.2740 \\ L_1 & 0 & 0 & 0.2560 & 0 & 0.005 & 0 \\ L_2 & 0 & 0 & 0.003 & 0 & 0.2740 & 0 \end{bmatrix} \quad (1)$$

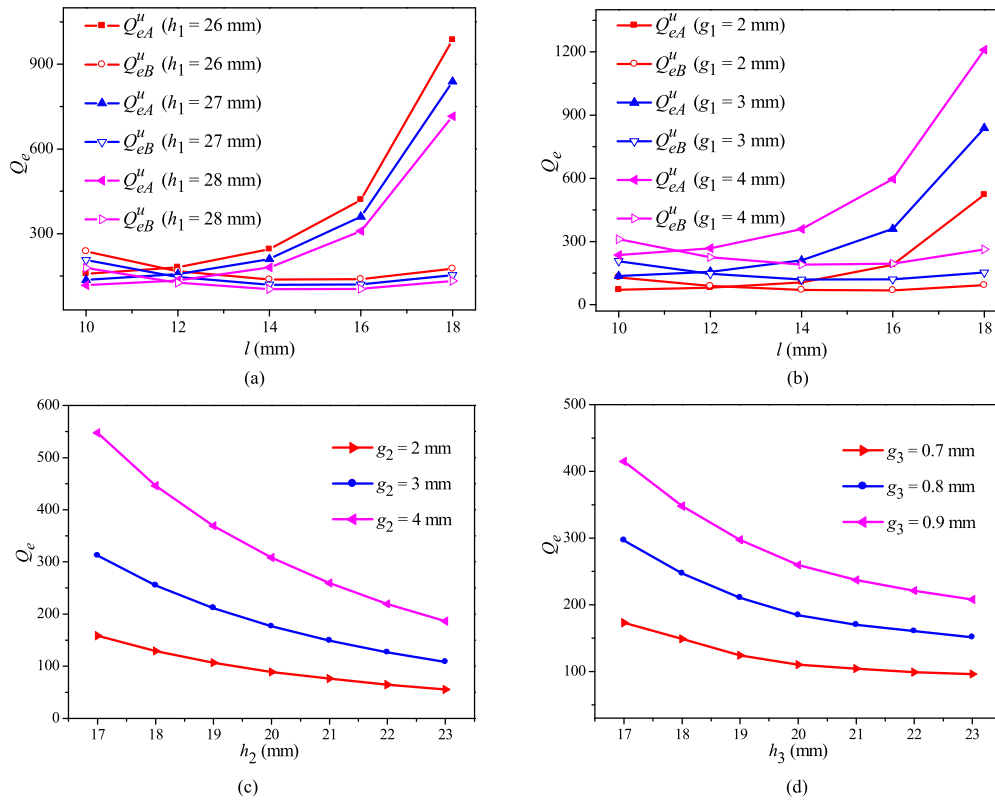


FIGURE 6. (a) Single-ended Q_e versus l with different h_1 ($g_1 = 3$ mm); (b) Single-ended Q_e versus l with different g_1 ($h_1 = 27$ mm); (c) Q_e versus h_2 with different g_2 ; (d) Q_e versus h_3 with different g_3 .

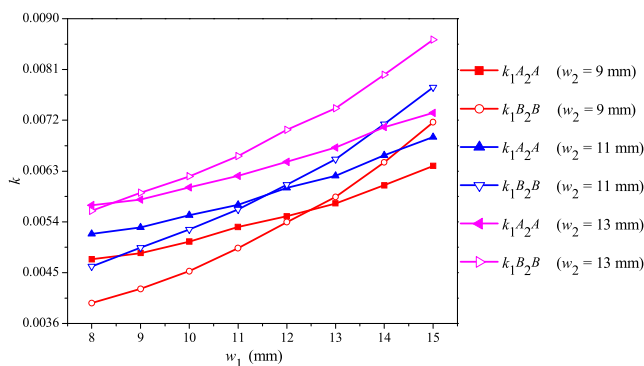


FIGURE 7. k versus w_1 with different w_2 .

The simulated and measured isolations (S_{23}) are better than 34 dB and 33 dB, respectively.

The comparisons with other diplexers are summarized in Table 1. As can be seen, this work shows many advantages such as low insertion loss, small size and minimum fractional bandwidth (FBW). Compared with the other 3-D structures using the T-junction [26], [27], [34], [35] and the star-junction [36], the design of full dual-mode DR can achieve the size reduction. Compared with the other implementations that need 2 coupling matrices to synthesize the two bands separately, only one coupling matrix is used in this design, which improves the design efficiency.

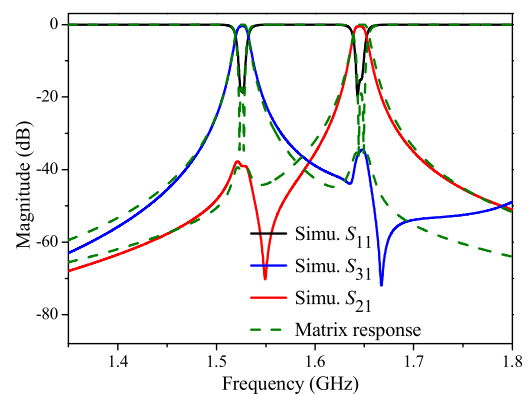


FIGURE 8. Frequency response generated by the coupling matrix M and the simulation results.

IV. BALANCED-TO-UNBALANCED DIPLEXER

The topology of the B2U diplexer is shown in Fig. 10. Based on the U2U diplexer, the B2U diplexer can be achieved by adding an additional port to the input port to form a balanced input port. In this design, the Q_e of the two kinds of input ports must satisfy $Q_{eA}^b = Q_{eA}^u$ and $Q_{eB}^b = Q_{eB}^u$ [23], [33]. This can be achieved by only changing the probe length of the balanced input port while other parameters are the same as the U2U counterpart. Fig. 11 shows the extracted Q_e of the balanced input under the two modes (Q_{eA}^b and Q_{eB}^b) versus

TABLE 1. Comparisons with previous diplexers.

Ref.	f_1/f_2 (GHz)	Types	Coupling junction	Analysis method	3-dB FBW(%)	Insertion Loss (dB)	Isolation (dB)	Size
[7]	5/5.25	SIW	T-junction	2 coupling matrices	1.95/2.08	2.2/2.4	45	$1.25*0.62(\lambda_0^2)$
[12]	1/1.8	Coaxial	None	2 coupling matrices	16/6	0.72/0.55	50	$0.873*0.263*0.167(\lambda_0^3)$
[14]	2.41/3.61	Microstrip	None	Even-/odd-mode & 2 coupling matrices	3.82/6.0	1.46/2.15	38	$0.25*0.06(\lambda_0^2)$
[26]	2.55/2.66	DR	T-junction	2 coupling matrices	3.8/3.5	0.63/1.10	20	$1.02 * 0.51 * 0.51(\lambda_0^3)$
[27]	2.54/2.67	DR	T-junction	2 coupling matrices	2.76/2.25	0.96/1.22	50	$1.02 * 1.02 * 0.51(\lambda_0^3)$
[34]	1.793/2.055	Coaxial	T-junction	2 coupling matrices	9.5/13.6	0.7/0.55	34	$0.81*0.36*0.18(\lambda_0^3)$
[35]	3.4/4.7	Waveguide	T-junction	Equivalent circuit	29.4/21.3	0.9	30	$1.17*0.61*0.082(\lambda_0^3)$
[36]	2.523/2.669	Coaxial	Star-junction	1 coupling matrix	3.6/3.7	0.6/0.6	50	$0.798*0.487*0.21(\lambda_0^3)$
This work	1.52/1.64	DR	None	1 coupling matrix	0.85/1.1	0.8/0.5	33	$0.42*0.20*0.16(\lambda_0^3)$

λ_0 : the wavelength at f_1 in the free space.

TABLE 2. Comparisons with previous balun diplexers.

Ref.	f_1/f_2 (GHz)	Types	Port Type	3-dB FBW(%)	Insertion Loss (dB)	Isolation (dB)	CMR(dB)	Size
[11]	2.2/2.8	SIW	U2B	2.7/1.7	2.2/2.7	28	44	$0.44*0.32(\lambda_0^2)$
[18]	2.61/2.78	Metal cavity	B2U	1.1/1.5	0.7/0.6	27	32	$1.65*1.22*0.70(\lambda_0^3)$
This work	1.52/1.64	DR	B2U	0.65/0.92	0.65/0.67	26	22/30	$0.42*0.20*0.16(\lambda_0^3)$

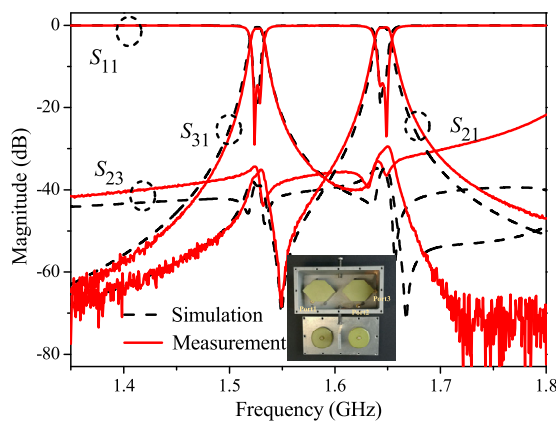


FIGURE 9. Simulated and measured S-parameters and isolations of the U2U diplexer.

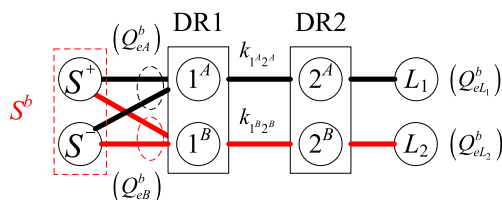


FIGURE 10. Topology of the B2U diplexer.

probe length h with different gap g . The dimensions of the probe length and gap after optimization can be determined as $g_1 = 3.1$ mm and $h_1 = 22.3$ mm.

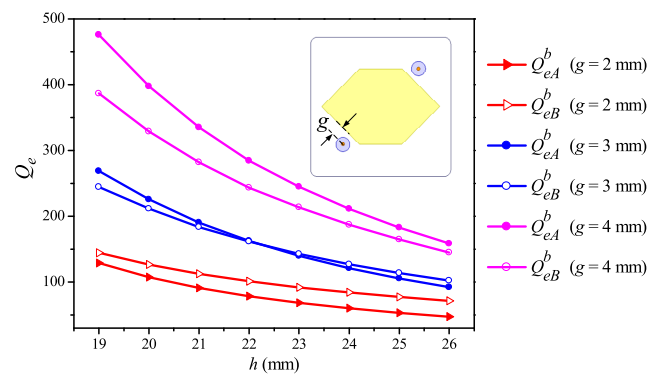


FIGURE 11. Differential Q_e versus h with different g_1 .

The simulated and measured results of the B2U diplexer are shown in Figs. 12(a)-(b). The simulated and measured center frequencies of the dual bands are 1.52 GHz and 1.64 GHz, respectively. The simulated return losses of the dual bands are larger than 15.9 dB and 15 dB. The measured dual-band return losses of them are larger than 14.27 dB and 14.31 dB. The simulated dual-band insertion losses are both less than 0.53 dB and the measured dual-band insertion losses are both less than 0.67 dB. The simulated and measured isolations are better than 33 dB and 26 dB, respectively. The simulated and measured common-mode rejections (CMR) are better than 31 dB and 22 dB, respectively. The difference

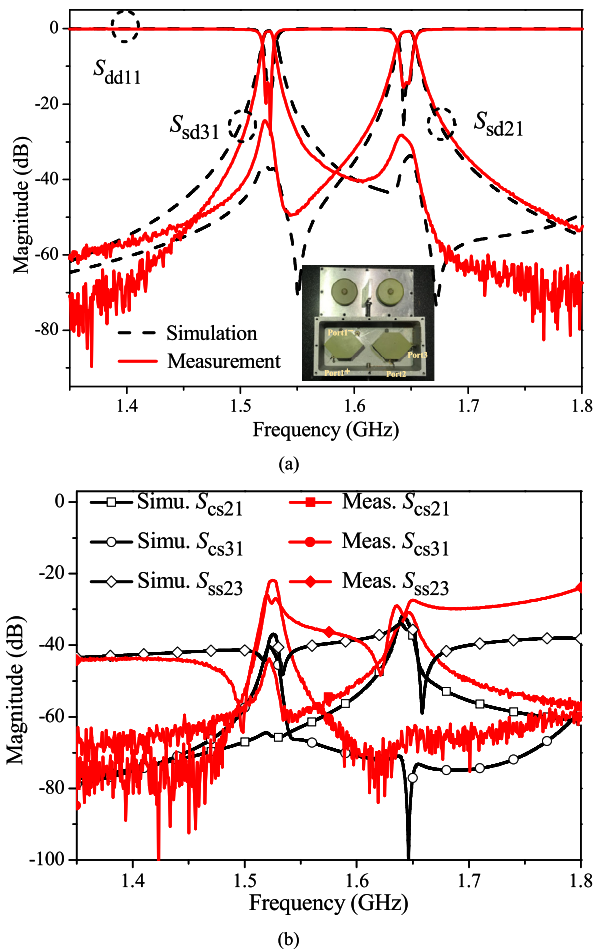


FIGURE 12. (a) Simulated and measured S-parameters of the B2U diplexer; (b) Simulated and measured isolations and CMRs of the B2U diplexer.

between the simulated and measured results can be due to the fabrication errors, the measuring errors and the loss of the SMA connectors.

Table 2 shows the comparisons with other balun diplexers. The same with the U2U diplexer proposed above, the B2U diplexer also has the lowest insertion loss in the case of minimum FBW, showing good passband performance.

V. CONCLUSION

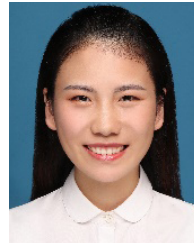
In this paper, we proposed the compact U2U and B2U diplexers. By using dual-mode DR, the circuit size is effectively reduced. Since the Q_e of two modes can be controlled independently, the design procedure is simple and efficient. The proposed U2U and B2U diplexers can be easily built by properly adding feeding probes for the DR without increasing the circuit size by altering the location of the feeding probes according to the distribution of the electromagnetic fields. Both of the two prototypes are verified by the simulation and experiment. Good performance, such as low insertion loss, high selectivity, and compact structure, has been realized, which makes the diplexer attractive in modern wireless communication systems. If wider bandwidth

is required, higher filtering orders can be considered properly.

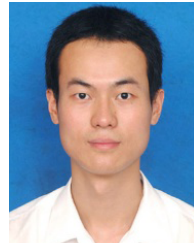
REFERENCES

- [1] P.-H. Deng, S.-W. Lei, W. Lo, and M.-W. Li, "Novel diplexer and triplexer designs avoiding additional matching circuits outside filters," *IEEE Access*, vol. 8, pp. 14714–14723, Jan. 2020.
- [2] L. Nouri, S. Yahya, and A. Rezaei, "Design and fabrication of a low-loss microstrip lowpass-bandpass diplexer for WiMAX applications," *China Commun.*, vol. 17, no. 6, pp. 109–120, Jun. 2020.
- [3] Q. Duan, K. Song, F. Chen, and Y. Fan, "Compact wide-stopband diplexer using dual mode resonators," *Electron. Lett.*, vol. 51, no. 14, pp. 1085–1087, Jul. 2015.
- [4] F. Cheng, X. Q. Lin, Z. B. Zhu, L. Y. Wang, and Y. Fan, "High isolation diplexer using quarter-wavelength resonator filter," *Electron. Lett.*, vol. 48, no. 6, pp. 330–331, Mar. 2012.
- [5] S. Sirci, J. D. Martinez, J. Vague, and V. E. Boria, "Substrate integrated waveguide diplexer based on circular triplet combine filters," *IEEE Microw. Wireless Compon. Lett.*, vol. 25, no. 7, pp. 430–432, Jul. 2015.
- [6] T. Zheng, B. Wei, B. Cao, X. Guo, X. Zhang, L. Jiang, Z. Xu, and Y. Heng, "Compact superconducting diplexer design with conductor-backed coplanar waveguide structures," *IEEE Trans. Appl. Supercond.*, vol. 25, no. 2, pp. 1–4, Apr. 2015.
- [7] K. Song, Y. Zhou, Y. Chen, A. Mohamed Iman, S. Richard Patience, and Y. Fan, "High-isolation diplexer with high frequency selectivity using substrate integrate waveguide dual-mode resonator," *IEEE Access*, vol. 7, pp. 116676–116683, Jul. 2019.
- [8] Q.-Y. Lu, Y.-J. Zhang, J. Cai, W. Qin, and J.-X. Chen, "Microstrip tunable diplexer with separately-designable channels," *IEEE Trans. Circuits Syst. II, Exp. Briefs*, vol. 67, no. 12, pp. 2983–2987, Dec. 2020.
- [9] K. Zhou, C.-X. Zhou, and W. Wu, "Compact SIW diplexer with flexibly allocated bandwidths using common dual-mode cavities," *IEEE Microw. Wireless Compon. Lett.*, vol. 28, no. 4, pp. 317–319, Apr. 2018.
- [10] H.-W. Xie, K. Zhou, C.-X. Zhou, and W. Wu, "Compact SIW diplexers and dual-band bandpass filter with wide-stopband performances," *IEEE Trans. Circuits Syst. II, Exp. Briefs*, vol. 67, no. 12, pp. 2933–2937, Dec. 2020.
- [11] M. F. Hagag, M. Abu Khater, M. D. Hickie, and D. Peroulis, "Tunable SIW cavity-based dual-mode diplexers with various single-ended and balanced ports," *IEEE Trans. Microw. Theory Techn.*, vol. 66, no. 3, pp. 1238–1248, Mar. 2018.
- [12] Y. Xie, F.-C. Chen, Q.-X. Chu, and Q. Xue, "Dual-band coaxial filter and diplexer using stub-loaded resonators," *IEEE Trans. Microw. Theory Techn.*, vol. 68, no. 7, pp. 2691–2700, Jul. 2020.
- [13] Q. Xue and J.-X. Chen, "Compact diplexer based on double-sided parallel-strip line," *Electron. Lett.*, vol. 44, no. 2, pp. 123–124, Jan. 2008.
- [14] J.-K. Xiao, M. Zhang, and J.-G. Ma, "A compact and high-isolated multiresonator-coupled diplexer," *IEEE Microw. Wireless Compon. Lett.*, vol. 28, no. 11, pp. 999–1001, Nov. 2018.
- [15] Y. C. Li, D.-S. Wu, Q. Xue, and B.-J. Hu, "Miniaturized single-ended and balanced dual-band diplexers using dielectric resonators," *IEEE Trans. Microw. Theory Techn.*, vol. 68, no. 10, pp. 4257–4266, Oct. 2020.
- [16] X. Guan, F. Yang, H. Liu, and L. Zhu, "Compact and high-isolation diplexer using dual-mode stub-loaded resonators," *IEEE Microw. Wireless Compon. Lett.*, vol. 24, no. 6, pp. 385–387, Jun. 2014.
- [17] F. Cheng, X. Lin, K. Song, Y. Jiang, and Y. Fan, "Compact diplexer with high isolation using the dual-mode substrate integrated waveguide resonator," *IEEE Microw. Wireless Compon. Lett.*, vol. 23, no. 9, pp. 459–461, Sep. 2013.
- [18] S.-W. Wong, J.-Y. Lin, H. Zhu, R.-S. Chen, L. Zhu, and Y. He, "Cavity balanced and unbalanced diplexer based on triple-mode resonator," *IEEE Trans. Ind. Electron.*, vol. 67, no. 6, pp. 4969–4979, Jun. 2020.
- [19] J.-Y. Lin, S.-W. Wong, Y.-M. Wu, L. Zhu, Y. Yang, and Y. He, "A new concept and approach for integration of three-state cavity diplexer based on triple-mode resonators," *IEEE Trans. Microw. Theory Techn.*, vol. 66, no. 12, pp. 5272–5279, Dec. 2018.
- [20] X. Q. Lin, J. Y. Jin, J. W. Yu, Y. Jiang, Y. Fan, and Q. Xue, "Design and analysis of EMIT filter and diplexer," *IEEE Trans. Ind. Electron.*, vol. 64, no. 4, pp. 3059–3066, Apr. 2017.
- [21] J. O. Garcia, J. C. M. Lernas, S. Cogollos, V. E. Boria, and M. Guglielmi, "Waveguide quadruplet diplexer for multi-beam satellite applications," *IEEE Access*, vol. 8, pp. 110116–110128, Jun. 2020.

- [22] X. Y. Zhang and J.-X. Xu, "Multifunctional filtering circuits: 3D multifunctional filtering circuits based on high-Q dielectric resonators and coaxial resonators," *IEEE Microw. Mag.*, vol. 21, no. 3, pp. 50–68, Mar. 2020.
- [23] W. Yu, W. Qin, and J.-X. Chen, "Theory and experiment of multipoint filtering power divider with arbitrary division ratio based on dielectric resonator," *IEEE Trans. Ind. Electron.*, vol. 66, no. 1, pp. 407–415, Jan. 2019.
- [24] J.-X. Chen, Y. Zhan, W. Qin, and Z.-H. Bao, "Design of high-performance filtering balun based on TE_{01δ}-mode dielectric resonator," *IEEE Trans. Ind. Electron.*, vol. 64, no. 1, pp. 451–458, Jan. 2017.
- [25] L.-H. Zhou, J.-X. Chen, and Q. Xue, "Design of compact coaxial-like bandpass filters using dielectric-loaded strip resonator," *IEEE Trans. Compon., Packag., Manuf. Technol.*, vol. 8, no. 3, pp. 456–464, Mar. 2018.
- [26] S.-W. Wong, Z.-C. Zhang, S.-F. Feng, F.-C. Chen, L. Zhu, and Q.-X. Chu, "Triple-mode dielectric resonator diplexer for base-station applications," *IEEE Trans. Microw. Theory Techn.*, vol. 63, no. 12, pp. 3947–3953, Dec. 2015.
- [27] Z.-C. Zhang, Q.-X. Chu, S.-W. Wong, S.-F. Feng, L. Zhu, Q.-T. Huang, and F.-C. Chen, "Triple-mode dielectric-loaded cylindrical cavity diplexer using novel packaging technique for LTE base-station applications," *IEEE Trans. Compon., Packag., Manuf. Technol.*, vol. 6, no. 3, pp. 383–389, Mar. 2016.
- [28] H.-W. Deng, T. Xu, Y.-F. Xue, F. Liu, and L. Sun, "Closely spaced broadband MIMO differential filtering slotline antenna with CM suppression," *IEEE Antennas Wireless Propag. Lett.*, vol. 17, no. 12, pp. 2498–2502, Dec. 2018.
- [29] K. Sun, Y. Zhao, D. Yang, and J. Pan, "A single-layer differential substrate-integrated slot antenna with common-mode rejection," *IEEE Antennas Wireless Propag. Lett.*, vol. 18, no. 2, pp. 392–396, Feb. 2019.
- [30] L.-H. Wen, S. Gao, Q. Luo, Q. Yang, W. Hu, Y. Yin, J. Wu, and X. Ren, "A wideband series-fed circularly polarized differential antenna by using crossed open slot-pairs," *IEEE Trans. Antennas Propag.*, vol. 68, no. 4, pp. 2565–2574, Apr. 2020.
- [31] F. Huang, J. Wang, L. Zhu, and W. Wu, "Compact microstrip balun diplexer using stub-loaded dual-mode resonators," *Electron. Lett.*, vol. 52, no. 24, pp. 1994–1996, Nov. 2016.
- [32] C.-M. Chen, S.-J. Chang, C.-F. Yang, and C.-Y. Chen, "A simple and effective method for designing frequency adjustable balun diplexer with high common-mode suppression," *IEEE Microw. Wireless Compon. Lett.*, vol. 25, no. 7, pp. 433–435, Jul. 2015.
- [33] Q. Xue, J. Shi, and J.-X. Chen, "Unbalanced-to-balanced and balanced-to-unbalanced diplexer with high selectivity and common-mode suppression," *IEEE Trans. Microw. Theory Techn.*, vol. 59, no. 11, pp. 2848–2855, Nov. 2011.
- [34] Z. Qi, X. Li, and J. Zeng, "Wideband diplexer design and optimization based on back-to-back structured common port," *IEEE Microw. Wireless Compon. Lett.*, vol. 28, no. 4, pp. 320–322, Apr. 2018.
- [35] B.-L. Zheng, S.-W. Wong, S.-F. Feng, L. Zhu, and Y. Yang, "Multi-mode bandpass cavity filters and diplexer with slot mixed-coupling structure," *IEEE Access*, vol. 6, pp. 16353–16362, Oct. 2018.
- [36] P. Zhao and K.-L. Wu, "An iterative and analytical approach to optimal synthesis of a multiplexer with a star-junction," *IEEE Trans. Microw. Theory Techn.*, vol. 62, no. 12, pp. 3362–3369, Dec. 2014.



LIN XU was born in Nantong, Jiangsu, China, in 1997. She received the B.S. degree from Nantong University, Nantong, in 2019, where she is currently pursuing the M.S. degree in electromagnetic field and microwave technology. Her current research interest includes microwave circuits.



WEI YU was born in Nantong, Jiangsu, China, in 1986. He received the B.S. and M.S. degrees from Nanjing Forestry University, Nanjing, China, in 2009 and 2012, respectively. He is currently pursuing the Ph.D. degree in information and communication engineering with Nantong University, Nantong.

Since 2012, he has been with the Engineering Training Center, Nantong University, where he is also a Lecturer. His research interest includes microwave active/passive circuits and antennas.



JIAN-XIN CHEN (Senior Member, IEEE) was born in Nantong, Jiangsu, China, in 1979. He received the B.S. degree from the Huai Yin Teachers College, Jiangsu, in 2001, the M.S. degree from the University of Electronic Science and Technology of China (UESTC), Chengdu, China, in 2004, and the Ph.D. degree from the City University of Hong Kong, Hong Kong, in 2008.

Since 2009, he has been with Nantong University, where he is currently a Professor. He has authored or coauthored more than 80 internationally refereed journal and conference papers. He holds three Chinese patents and two U.S. patents. His research interests include microwave active/passive circuits and antennas and LTCC-based millimeter-wave circuits and antennas. He was a recipient of the Best Paper Award presented at the Chinese National Microwave and Millimeter-Wave Symposium, Ningbo, China, in 2007. He was a Supervisor of the 2014 iWEM Student Innovation Competition Winner in Sapporo, Japan.

• • •